RCO-2010-001

PERSONAL DOSE EQUIVALENT CONVERSION COEFFICIENTS FOR PHOTONS TO 1 GEV

K. G. Veinot[1], N.E. Hertel[2]

[1]Y-12 National Security Complex
P.O. Box 2009, M.S. 8105
Oak Ridge, TN 37831-8105
veinotkg@y12.doe.gov
865-241-6165 (Phone)
865-241-2016 (Fax)

[2]George W. Woodruff School of Mechanical Engineering
Georgia Institute of Technology
Atlanta, Georgia 30332-0405
nolan.hertel@me.gatech.edu

09/27/2010

Running Title: Photon Dose Conversion Coefficients

Personal Dose Equivalent Conversion Coefficients for Photons to 1 GeV

K. G. Veinot, N.E. Hertel

ABSTRACT

The personal dose equivalent, $H_p(d)$, is the quantity recommended by the International Commission on Radiation Units and Measurements (ICRU) to be used as an approximation of the protection quantity Effective Dose when performing personal dosemeter calibrations. The personal dose equivalent can be defined for any location and depth within the body. Typically, the location of interest is the trunk where personal dosemeters are usually worn and in this instance a suitable approximation is a 30 cm X 30 cm X 15 cm slab-type phantom. For this condition the personal dose equivalent is denoted as $H_{p,slab}(d)$ and the depths, d, are taken to be 0.007 cm for non-penetrating and 1 cm for penetrating radiation. In operational radiation protection a third depth, 0.3 cm, is used to approximate the dose to the lens of the eye. A number of conversion coefficients for photons are available for incident energies up to several MeV, however, data to higher energies are limited. In this work conversion coefficients up to 1 GeV have been calculated for $H_{p,slab}(10)$ and $H_{p,slab}(3)$ using both the kerma approximation and by tracking secondary charged particles. For $H_p(0.07)$ the conversion coefficients were calculated, but only to 10 MeV due to computational limitations. Additionally, conversions from air kerma to $H_{p,slab}(d)$ have been determined and are reported. The conversion coefficients were determined for discrete incident energies, but analytical fits of the coefficients over the energy range are provided. Since the inclusion of air can influence the production of secondary charged particles incident on the face of the phantom conversion coefficients have been determined both *in vacuo* and with the source and slab immersed within a sphere in air. The conversion coefficients for the personal dose equivalent are compared to the appropriate protection quantity, calculated

according to the recommendations of the latest International Commission on Radiological Protection (ICRP) guidance.

Personal Dose Equivalent Conversion Coefficients to 1 GeV

INTRODUCTION

The personal dose equivalent, $H_p(d)$, is the quantity recommended by the International Commission on Radiation Units and Measurements (ICRU) to be used as an approximation of the protection quantity Effective Dose [1, 2]. The personal dose equivalent can be defined for any location and depth within the body although three specific depths are typically used for radiation protection settings, namely 0.007 cm, 0.3 cm, and 1 cm. When performing dosemeter calibrations the location of interest is typically the trunk and in this instance a suitable approximation is a 30 cm X 30 cm X 15 cm slab-type phantom. For this condition the personal dose equivalent is denoted as $H_{p,slab}(d)$ and the depths, d, are taken to be 0.007 cm for non-penetrating and 1 cm for penetrating radiation. In operational radiation protection a third depth, 0.3 cm, is included to approximate the lens of the eye. Although non-penetrating radiation is commonly quoted as relevant, penetrating radiation also contributes to $H_p(0.07)$.

A number of conversion coefficients for photons are available for incident energies up to several MeV (for example references 3 – 6), however, data to higher energies are limited especially for personal dose equivalent. Additionally, the assumptions and modeling conditions chosen by the authors differ as do the computational codes used. In this work conversion coefficients have been calculated in a 30 cm X 30 cm X 15 cm slab-type phantom constructed of ICRU tissue substitute. Absorbed dose calculations were performed at depths of 0.007 cm, 0.3 cm, and 1 cm since these depths are used as approximations of skin equivalent dose, eye lens equivalent dose, and

effective dose, respectively. The range of energies considered spans from 0.002 MeV to 10 MeV for d = 0.007 cm and to 1 GeV for depths of 0.3 cm and 1 cm. The limit of 10 MeV for $H_p(0.07)$ was a result of the small scoring volume used in the simulations which led to prohibitively long computational times at higher energies.

As has been discussed in various papers as well as ICRU reports [1] the inclusion or omission of air in the region between the simulated source and the phantom can have significant impacts on the establishment of charged particle equilibrium (CPE), particularly at the 0.007 cm depth. The impact of the presence of air was investigated by performing the calculations in a vacuum and with the source modeled one meter from the phantom face enclosed by a sphere of air with radius of two meters. Since discrete energies were used in the calculations, analytical fits are provided for each data set to allow interpolation of values at other energies. The operational quantities are compared to the corresponding protection quantities determined according to the latest recommendations of the ICRP [2].

METHODOLOGY

Two sets of dose conversion coefficients were calculated using the Monte-Carlo transport code MCNPX version 2.6.0 [7]. For these calculations all secondary particles included in the code were tracked and their energy deposition tallied. Additionally, a kerma calculation was performed within each volume of interest. The quality factor was assumed to be unity regardless of the secondary particle produced. Further work may be needed since the production of heavy

charged particles and neutrons (having high LET values) occur at higher energies and would have quality factors exceeding unity.

The model consisted of a parallel broad beam of photons impinging perpendicular to the front face of a 30 cm X 30 cm X 15 cm slab-type phantom consisting of ICRU tissue substitute (10.1% hydrogen, 11.1% carbon, 2.6% nitrogen, 76.2% oxygen). The source beam was sufficiently large (radius of 22 cm) to fully illuminate the phantom face. Deposition calculations were performed within a 0.001 cm thick volume centered at a depth of 0.007 cm for $H_p(0.07)$ and within a 0.01 cm thick volume for $H_p(3)$ and $H_p(10)$. The scoring volume was defined as a cylinder having radius equal to 5 cm and thickness quoted above. Sufficient particle histories were generated so that the tally errors were less than 5%. When air was included the source was placed a distance of 100 cm from the front face, since this is a common distance used in dosemeter calibrations. All appropriate physics models were included (e.g. Bremsstrahlung, neutron production, etc.). Since the photoneutron production algorithm for higher energies was enabled, the $S(\alpha,\beta)$ thermal neutron treatment was included for neutron transport. The Cascade-Exciton Model (CEM) version CEM03 [7] was used for all energies.

Photon conversion coefficients are commonly reported in terms of the air kerma. The coefficients reported here are in units of pSv cm^2, but air kerma coefficients for each of the reported energies were computed by determining the kerma within an air sphere and these results are also provided.

To allow for determination of conversion coefficients at energies other than those calculated here analytical fits are provided. These fits were performed using a nonlinear least-squares Marquardt-Levenberg algorithm. Fits are of the form

$$f(x) = \frac{a}{1+(b+cx)^2} + \frac{d}{1+(f+gx)^2} + \frac{h}{1+(j+kx)^2} + \frac{l}{1+\exp(m+nx)} + \frac{o}{1+\exp(p+qx)} \qquad (1)$$

where *f(x)* is the logarithmic (base 10) value of the conversion coefficient and *x* equals $\log_{10}(E)$ with *E* having energy units of MeV.

In order to compare the operational quantities with the protection quantities, the conversion coefficients for the equivalent dose to the skin, equivalent dose to the lens of the eye, and the effective dose are compared with the present calculations. The protection quantity calculations were performed using the phantoms described in ICRP-110 [8] according to the guidelines given in ICRP-103 [2]. The MCNPX code was used and phantoms were irradiated in a vacuum in the anterior-posterior (A-P) geometry. Additional details on these calculations will be given in a future paper. The reported organ conversion coefficients are the average of the male and female phantoms.

RESULTS AND DISCUSSION

The calculated conversion coefficients are listed in Table 1 and shown in Figures 1-5. Although values of $H_p(3)$ and $H_p(10)$ with air were calculated they did not differ significantly from those determined in the vacuum and are not reported. Table 2 lists the fitting constants for each of the quantities according to Equation 1 along with the sum of squares residuals (SSR) of the fits.

Table 3 lists the coefficients for $H_p(d)$ per unit air kerma. Comparisons of $H_p(10)$ to the ambient dose equivalent [1], $H^*(10)$, calculated in the 15 cm radius ICRU sphere are shown in Figure 3.

The impact of the inclusion of air in the model is evident in Figure 1 where at low energies the photons are sufficiently scattered to reduce their penetrating ability. CPE is maintained to slightly higher energies since electronic buildup occurs between the source and the phantom. The inclusion of this limited amount of air had virtually no effect for doses at depths of 0.3 cm and 1 cm in the phantom.

The values of $H_p(0.07)$ provide a reasonable approximation to the equivalent dose to the skin up to about 400 keV. Above these energies CPE is not met at this depth in the slab phantom while the phantoms of ICRP-110 continue to increase in equivalent dose owing to the portions of skin on the sides and back. The dimensions of the phantom voxels (2.08 mm X 2.08 mm X 8 mm for the male phantom and 1.875 mm X 1.875 mm X 5 mm for the female) do not allow tallies specifically at the 0.07 mm depth, so the size of the voxels themselves likely impacted the calculations as well. To approximately 1.5 MeV the lens of the eye equivalent dose is reasonably approximated by $H_p(3)$. Above these energies the protection quantity is almost twice that of the operational quantity. The effective dose is approximated conservatively by $H_p(10)$ to almost 4 MeV. The kerma, $K_p(10)$, is a conservative estimator of E at all energies considered.

At 1 GeV approximately 95% of the dose is delivered by secondary electrons. About 2% of the dose results from protons, 1% from deuterons, and the rest from various other particles including alpha particles, pions, helium-3 atoms, and tritons. This work did not investigate the impact on

dose equivalent arising from these high-LET particles since the quality factor for photons was assumed to be unity regardless of the secondary charged particles produced and their corresponding LET. This is similar to the method used by other authors.

CONCLUSION

The calculated conversion coefficients provide additional information for higher energy photons. Although it is unlikely that dosemeter calibrations would be performed at these high energies, they may be of use for accidental exposures. The values computed here agree well with those published for the ICRU sphere indicating that differences in the phantoms do not significantly impact the conversion coefficients, at least when the irradiations are performed along the principal axis of the phantom. The minor differences in the reported values of $H^*(10,0)$ and those for $H_p(10,0)$ reported here could be a result of variations in tally volumes, shape, and transport codes/cross sections used as well as uncertainties in the scoring results. The minimal impact of phantom size and shape indicates that evaluations of operational quantities (at least photons) could include reported values for $H_p(10)$ and $H^*(10)$. The inclusion of air has been discussed by other authors and introduces additional considerations. For example, in order to maintain CPE at a given depth the distance between the source and the phantom would need to be increased as the photon energies increase. This would then eliminate the desired additivity of the operational quantity as would varying the depth at which the dose is calculated (or measured). The personal dose equivalent does not provide a conservative estimator of the protection quantities above certain energies (300 keV for the skin, 1.5 MeV for the lens of the eye, and 4 MeV for effective dose) when calculated in a vacuum. In reality, however, pure

photon beams are not observed since there are often objects or source encapsulations that provide some additional buildup of secondary particles not to mention buildup in air. The analytical fits provide convenient methods for determining conversion coefficients for specific energies or spectra of photons.

REFFERENCES

1. International Commission on Radiation Units and Measurements (ICRU). *Conversion coefficients for use in radiological protection against external radiation.* ICRU Publication 57. Bethesda, MD, 1998.

2. International Commission on Radiological Protection (ICRP). *The 2007 Recommendations of the International Commission on Radiological Protection.* ICRP Publication 103. Annals of the ICRP Volume 37, 2007.

3. International Commission on Radiological Protection (ICRP). *Conversion coefficients for use in radiological protection against external radiation.* ICRP Publication 74. Oxford: Pergamon Press, 1996.

4. M. Pelliccioni. Overview of Fluence-to-Effective Dose and Fluence-toAmbient Dose Equivalent Conversion Coefficients for High Energy Radiation Calculated Using the FLUKA Code. *Radiation Protection Dosimetry*, 88, No. 4, pp. 279-297, 2000.

5. J.O. Kim and J.K. Kim. Dose Equivalent Per Unit Fluence Near the Surface of the ICRU Phantom by Including the Secondary Electron Transport for Photons. *Radiation Protection Dosimetry*, 83, No. 3, pp. 211-219, 1999.

6. A. Ferrari and M. Pelliccioni. On the Conversion Coefficients for Use in Radiological Protection Against External Radiation. *Radiation Protection Dosimetry*, 51, pp. 251-255, 1994.

7. MCNPX Ver. 2.6.0. Edited by D.B. Pelowicz, Los Alamos National Laboratory, 2008.

8. International Commission on Radiological Protection (ICRP). *Adult reference computational phantoms.* ICRP Publication 110. Annals of the ICRP Volume 39, April 2009.

Table 1. Personal Dose Equivalent, $H_p(d)$, tissue kerma, $K_p(d)$, and air kerma, K_a, conversion coefficients. Units are pSv cm^2 for $H_p(d)$ and $K_p(d)$ and pGy cm^2 for air kerma.

Energy	Vacuum						Air	
(MeV)	$K_p(0.07)$	$K_p(3)$	$K_p(10)$	$H_p(0.07)$	$H_p(3)$	$H_p(10)$	$H_p(0.07)$	K_a
0.002	3.116	---	---	3.087	---	---		45.19
0.0025	14.56	---	---	14.54	---	---	0.390	54.80
0.003	24.61	---	---	24.49	---	---	3.044	51.30
0.004	28.70	---	---	28.47	---	---	10.33	40.15
0.005	23.81	---	---	23.79	---	---	14.09	28.47
0.006	18.44	---	---	18.59	---	---	13.72	20.59
0.007	14.24	0.227	---	14.21	0.224	---	11.65	15.39
0.01	7.219	1.829	0.063	7.146	1.824	0.065	6.741	7.515
0.015	3.187	2.184	0.819	3.088	2.191	0.825	3.097	3.198
0.02	1.823	1.589	1.054	1.802	1.605	1.056	1.833	1.728
0.03	0.914	0.914	0.829	0.914	0.916	0.828	0.919	0.740
0.04	0.635	0.659	0.656	0.659	0.674	0.669	0.629	0.439
0.05	0.530	0.559	0.575	0.546	0.568	0.574	0.534	0.329
0.06	0.498	0.527	0.549	0.506	0.529	0.552	0.510	0.293
0.08	0.528	0.556	0.580	0.545	0.558	0.585	0.516	0.309
0.1	0.614	0.641	0.665	0.600	0.643	0.670	0.648	0.373
0.15	0.899	0.928	0.953	0.924	0.932	0.943	0.883	0.599
0.2	1.214	1.248	1.266	1.161	1.243	1.247	1.196	0.857
0.3	1.829	1.862	1.874	1.225	1.864	1.846	1.725	1.380
0.4	2.407	2.438	2.445	1.131	2.449	2.429	1.765	1.891
0.5	2.947	2.974	2.975	1.052	2.986	2.989	1.619	2.378
0.6	3.457	3.483	3.477	1.009	3.489	3.451	1.564	2.841
0.7	3.938	3.961	3.948	0.876	4.000	3.948	1.484	3.280
0.8	4.393	4.414	4.395	0.801	4.460	4.464	1.316	3.700
1	5.234	5.249	5.218	0.800	5.259	5.274	1.159	4.476
1.5	7.026	7.029	6.978	0.603	6.095	7.200	0.947	6.136
2	8.547	8.541	8.473	0.535	5.698	8.675	0.791	7.545
3	11.14	11.12	11.03	0.419	4.745	10.95	0.600	9.955
4	13.44	13.41	13.30	0.374	3.968	11.20	0.535	12.11
5	15.59	15.55	15.42	0.326	3.608	10.64	0.469	14.15
6	17.66	17.61	17.47	0.322	3.333	10.05	0.461	16.13
8	21.75	21.68	21.51	0.280	2.955	9.356	0.398	20.09
10	25.83	25.75	25.53	0.283	2.821	8.970	0.386	24.08
15	---	36.19	35.87	---	2.732	8.920	---	34.39
20	---	47.04	46.60	---	2.679	8.490	---	45.41
30	---	70.15	69.45	---	2.769	8.919	---	68.57
40	---	94.63	93.66	---	2.985	9.042	---	93.22
50	---	120.3	119.1	---	3.004	9.119	---	119.1
100	---	258.5	255.6	---	3.120	9.944	---	259.0
200	---	558.7	551.8	---	3.690	11.46	---	563.2
500	---	1511	1491	---	5.346	13.10	---	1528
1000	---	3138	3094	---	5.112	13.21	---	3177

Table 2. Analytical fit values for $H_p(d)$ and K_a/ϕ conversion coefficients. Variables coincide with those given in Equation 1. Also listed is the sum of squares of the residuals (SSR) of the fit to the calculated data points. The fits for each quantity should only be used for the energy ranges listed in Table 1.

	Vacuum						Air	
	$H_p(0.07)$	$H_p(3)$	$H_p(10)$	$K_p(0.07)$	$K_p(3)$	$K_p(10)$	$H_p(0.07)$	K_a
a	7.56727E+0	3.49792E+0	1.84527E+1	1.47207E+1	7.43420E-1	1.07884E+0	1.65364E+1	3.40172E+1
b	-5.01758E+0	2.48403E+0	2.44654E+0	3.69539E+0	-1.76800E-1	-9.42600E-2	9.34914E-1	1.15114E+0
c	-1.74882E+0	1.24532E+0	1.13121E+0	1.35651E+0	8.39647E-1	7.67418E-1	-1.92713E-2	3.64446E-1
d	-3.80312E+0	4.53282E-1	2.24280E-1	1.06940E+1	2.34672E+1	2.04921E+1	-1.43030E+1	5.08067E-1
f	1.08006E+0	-3.65885E-1	-1.37672E+0	1.92102E+0	1.52515E+0	1.62389E+0	-2.19297E+1	1.47395E+0
g	8.81955E-1	1.96823E+0	2.75534E+0	9.69996E-1	6.56462E-1	7.63055E-1	-7.66325E+0	2.01820E+0
h	-1.93108E+1	-1.69432E+0	-4.74686E-1	-1.08623E-1	-7.13456E-1	-2.92325E+0	4.92782E-2	1.03817E-1
j	6.25371E+0	2.86861E+1	3.12682E+1	2.89960E+1	3.06571E+1	3.00662E+1	3.91070E+1	2.58364E+1
k	1.92324E+0	1.28680E+1	1.53499E+1	1.17945E+1	1.41814E+1	1.42711E+1	1.73650E+1	1.47682E+1
l	9.26208E-1	-3.27833E+0	-4.45434E+1	-5.18752E+1	-5.68803E+1	-5.74098E+1	-3.81668E+0	-4.63041E+1
m	2.75850E+0	2.77034E+0	3.05231E+0	5.93399E-1	1.22949E+0	1.32599E+0	3.21608E+0	4.42619E-1
n	6.07307E+0	2.77349E+0	1.36356E+0	1.27994E-1	4.10212E-1	4.01796E-1	3.56510E+0	4.41972E-1
o	3.09856E+0	7.82285E-1	7.30902E-1	1.68181E+1	6.08023E+0	6.28007E+0	-9.76724E+0	4.60609E+0
p	-2.94462E-1	3.42397E+0	4.17571E+0	-2.84478E+0	-3.08000E+0	-3.32731E+0	-1.96769E+0	-1.82266E+0
q	2.34461E+0	-1.61818E+0	-2.00324E+0	-1.95935E+0	-2.79600E+0	-2.93032E+0	-1.25198E+0	-2.76015E+0
SSR	0.0038	0.0058	0.0010	0.0011	0.0001	0.0001	0.0040	0.0088

Table 3. Conversion coefficients for $H_p(d)$ in terms of the air kerma, K_a in units of Sv Gy^{-1}. Vacuum indicates the calculations were performed in a vacuum while "air" indicates the source and phantom were enclosed within a two meter radius sphere of air.

Energy (MeV)	Vacuum $H_p(0.07)/K_a$	Vacuum $H_p(3)/K_a$	Vacuum $H_p(10)/K_a$	Air $H_p(0.07)/K_a$
0.002	0.068	---	---	---
0.0025	0.265	---	---	0.007
0.003	0.477	---	---	0.059
0.004	0.709	---	---	0.257
0.005	0.836	---	---	0.495
0.006	0.903	---	---	0.667
0.007	0.924	0.015	---	0.757
0.01	0.951	0.243	0.009	0.897
0.015	0.966	0.685	0.258	0.969
0.02	1.043	0.928	0.611	1.060
0.03	1.236	1.239	1.119	1.243
0.04	1.500	1.535	1.524	1.433
0.05	1.659	1.725	1.746	1.623
0.06	1.728	1.806	1.884	1.743
0.08	1.764	1.808	1.894	1.672
0.1	1.608	1.726	1.799	1.739
0.15	1.542	1.554	1.572	1.473
0.2	1.355	1.451	1.456	1.397
0.3	0.888	1.350	1.337	1.250
0.4	0.598	1.295	1.285	0.933
0.5	0.442	1.256	1.257	0.681
0.6	0.355	1.228	1.215	0.551
0.7	0.267	1.220	1.204	0.452
0.8	0.217	1.205	1.207	0.356
1	0.179	1.175	1.178	0.259
1.5	0.098	0.993	1.173	0.154
2	0.071	0.755	1.150	0.105
3	0.042	0.477	1.100	0.060
4	0.031	0.328	0.925	0.044
5	0.023	0.255	0.752	0.033
6	0.020	0.207	0.623	0.029
8	0.014	0.147	0.466	0.020
10	0.012	0.117	0.373	0.016
15	---	0.079	0.259	---
20	---	0.059	0.187	---
30	---	0.040	0.130	---
40	---	0.032	0.097	---
50	---	0.025	0.077	---
100	---	0.012	0.038	---
200	---	0.007	0.020	---
500	---	0.003	0.009	---
1000	---	0.002	0.004	---

Captions

Fig. 1. Absorbed dose conversion coefficients for $H_p(0.07)$ in units of pSv cm^2. Results for both vacuum and with the inclusion of 100 cm of intervening air are shown along with the fits determined using the values in Table 2 according to Equation 1. Also shown are the values of $H_p(\mathit{0.07})$ given in Reference 4 and for the equivalent dose to the skin using the phantoms of ICRP-110.

Fig. 2. Absorbed dose conversion coefficients for $H_p(3)$ in units of pSv cm^2 along with the fit determined using the values in Table 2 according to Equation 1. Also shown are the values of $H_p(\mathit{3})$ given in Reference 4 and for the equivalent dose to the lens of the eye using the phantoms of ICRP-110.

Fig. 3. Absorbed dose conversion coefficients for $H_p(10)$ in units of pSv cm^2 along with the fit determined using the values in Table 2 according to Equation 1. Also shown are the values of $H_p(\mathit{10})$ given in Reference 4 and $H^*(\mathit{10})$ given in Reference 3 and for the effective dose using the phantoms of ICRP-110.

Fig. 4. Air kerma, K_a, conversion coefficients in units of pGy cm^2 and the fit determined using the values in Table 2 according to Equation 1. Also shown are the values listed in ICRP-74.

Fig. 5. Kerma conversion coefficients for 0.007 cm, 0.3 cm, and 1 cm depths in the slab phantom in units of pGy cm^2 and the fits determined using the values in Table 2 according to Equation 1. Also shown are the values of effective dose using the phantoms of ICRP-110 and the methodology described in ICRP-103.

Fig. 1. Absorbed dose conversion coefficients for $H_p(0.07)$ in units of pSv cm^2. Results for both vacuum and with the inclusion of 100 cm of intervening air are shown along with the fits determined using the values in Table 2 according to Equation 1. Also shown are the values of $H_p(\mathit{0.07})$ given in Reference 4 and for the equivalent dose to the skin using the phantoms of ICRP-110.

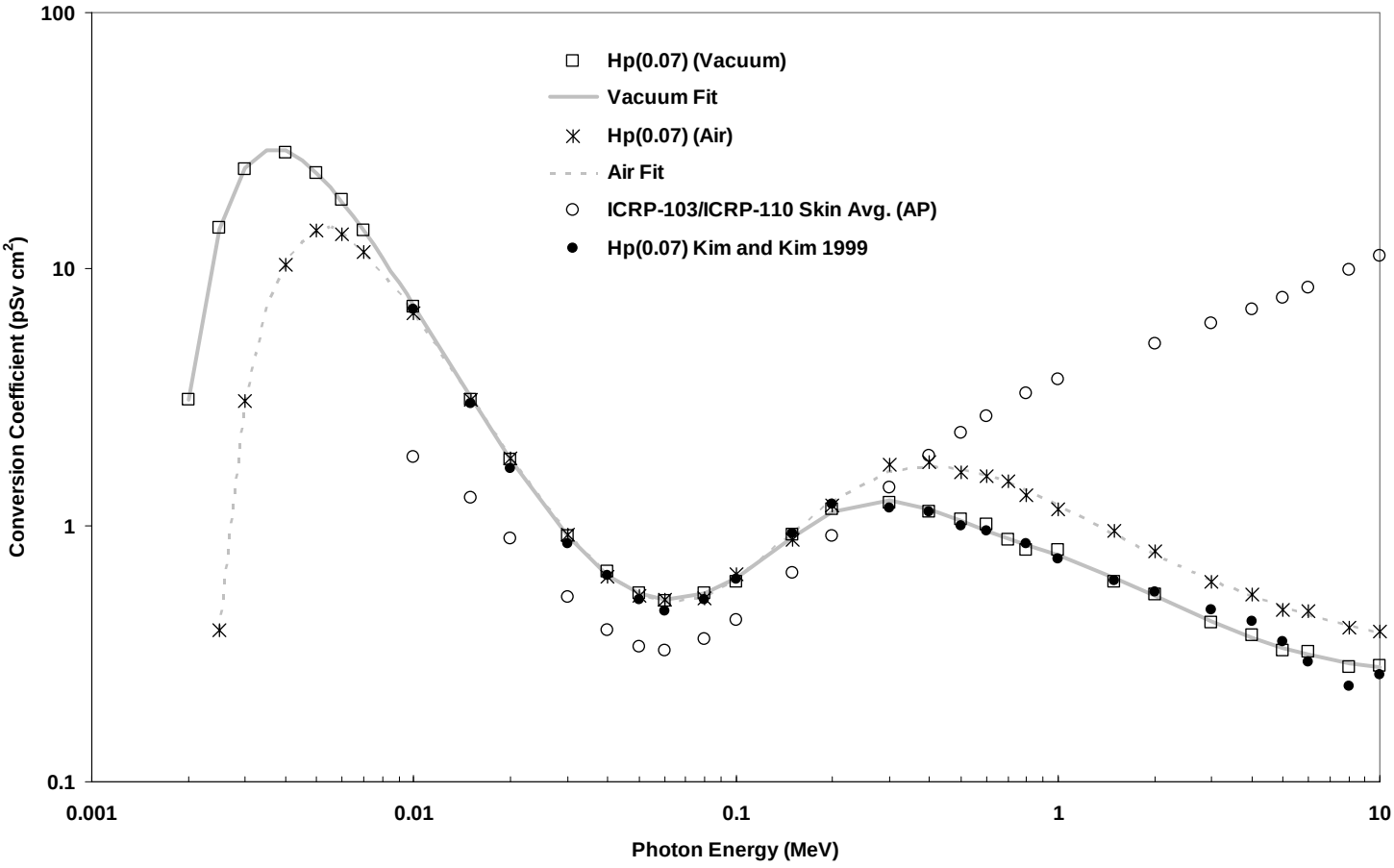

Fig. 2. Absorbed dose conversion coefficients for $H_p(3)$ in units of pSv cm^2 along with the fit determined using the values in Table 2 according to Equation 1. Also shown are the values of $H_p(3)$ given in Reference 4 and for the equivalent dose to the lens of the eye using the phantoms of ICRP-110.

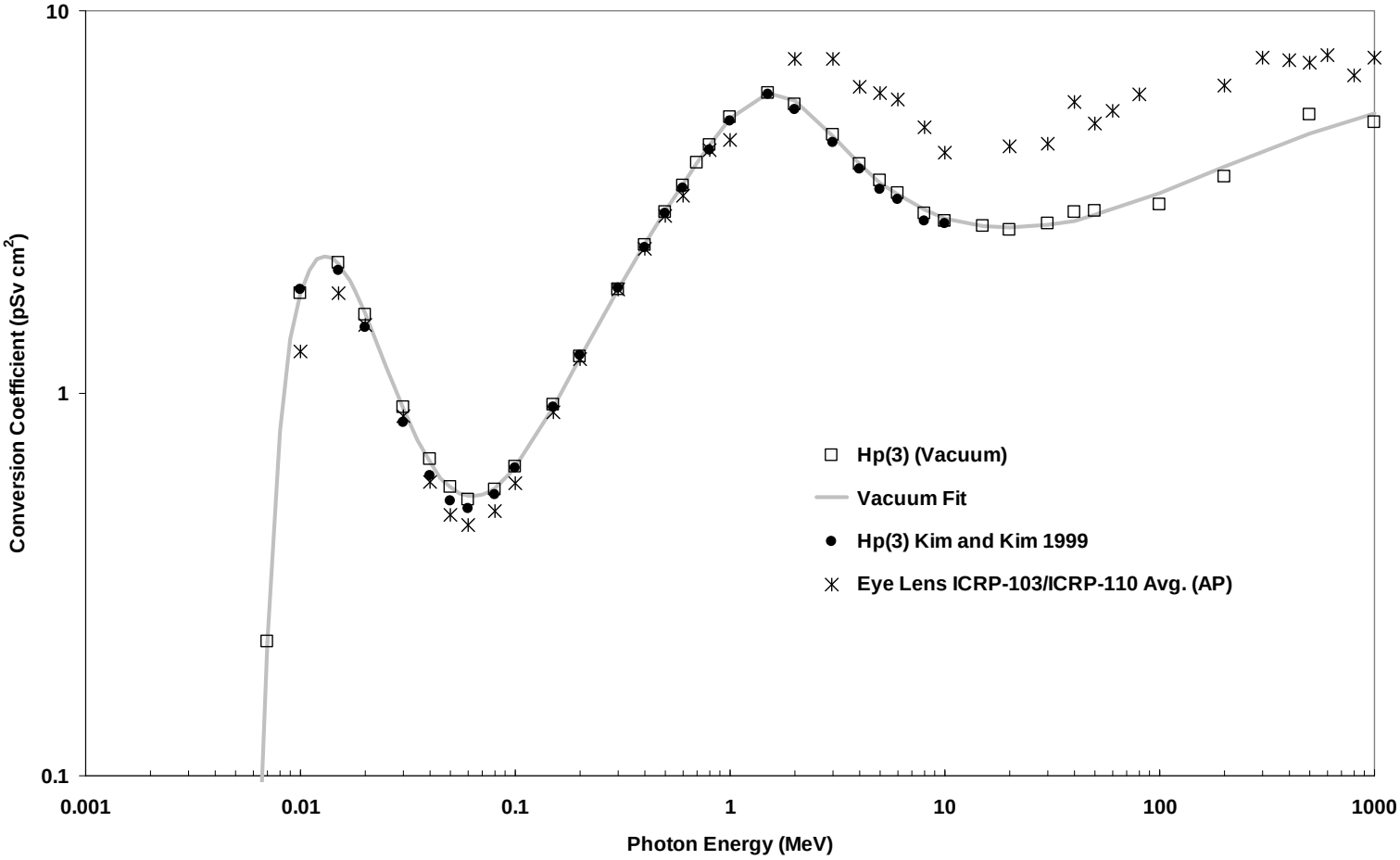

Fig. 3. Absorbed dose conversion coefficients for $H_p(10)$ in units of pSv cm^2 along with the fit determined using the values in Table 2 according to Equation 1. Also shown are the values of $H_p(10)$ given in Reference 4 and $H^*(10)$ given in Reference 3 and for the effective dose using the phantoms of ICRP-110.

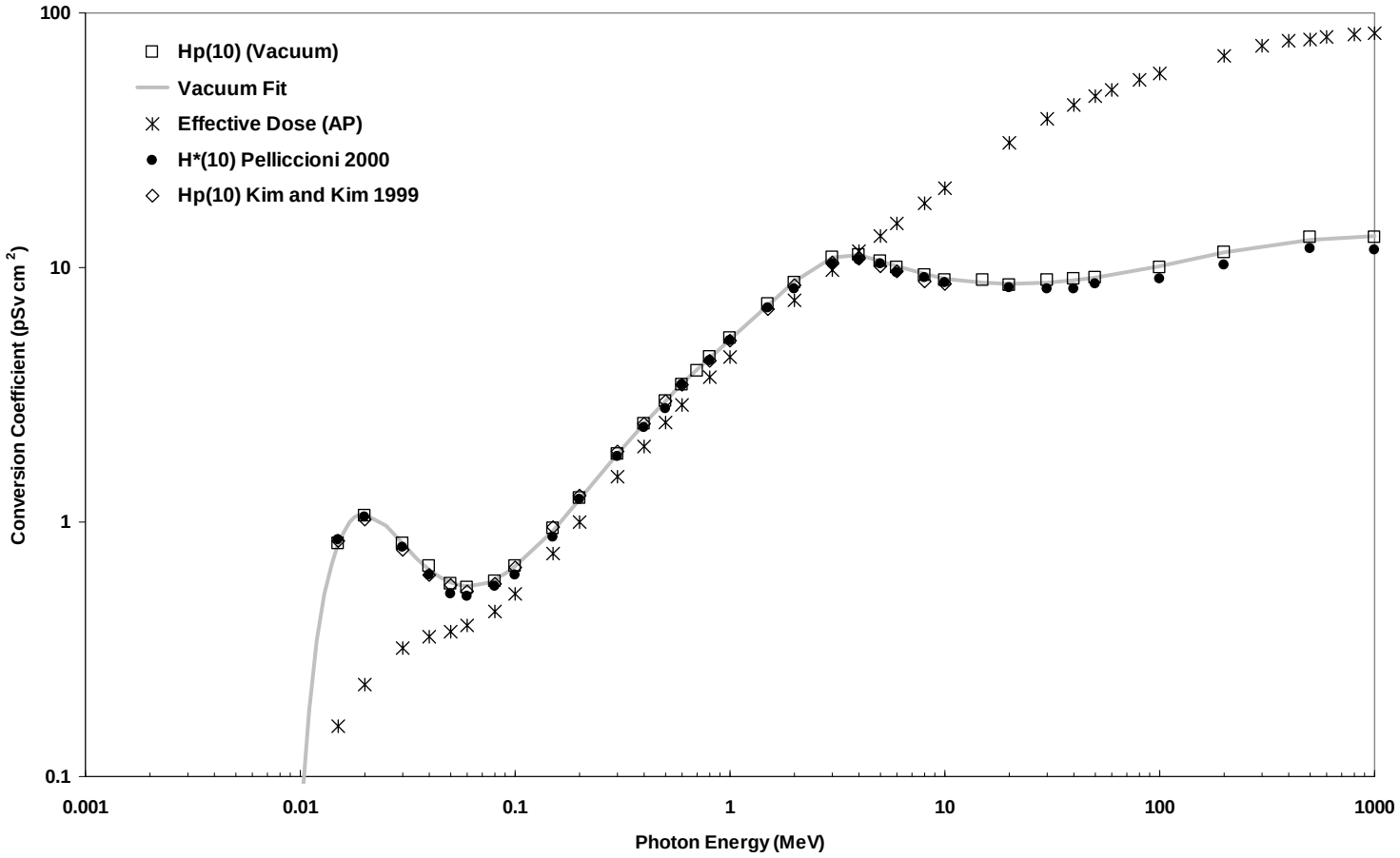

Fig. 4. Air kerma, K_a, conversion coefficients in units of pGy cm^2 and the fit determined using the values in Table 2 according to Equation 1. Also shown are the values listed in ICRP-74.

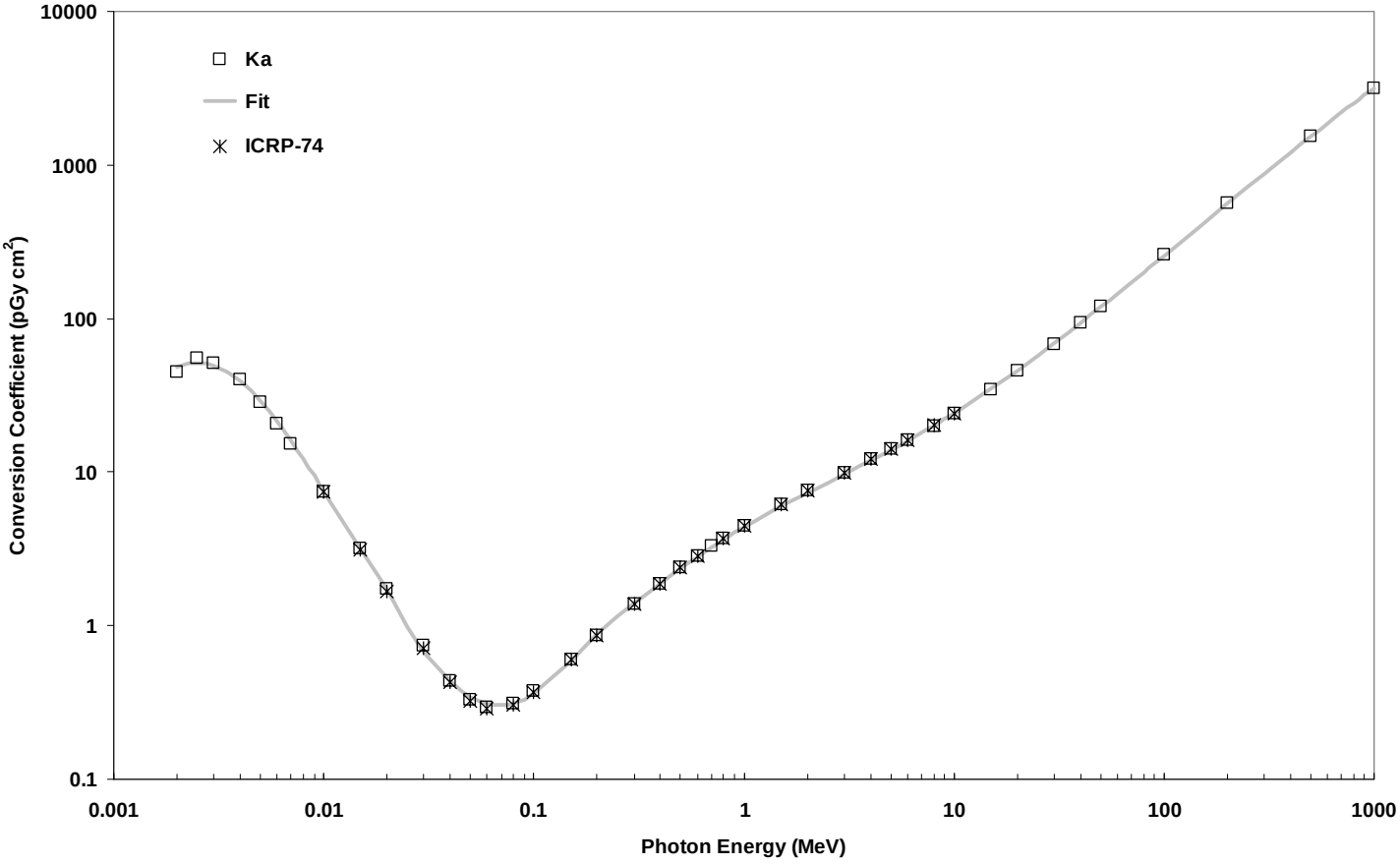

Fig. 5. Kerma conversion coefficients for 0.007 cm, 0.3 cm, and 1 cm depths in the slab phantom in units of pGy cm^2 and the fits determined using the values in Table 2 according to Equation 1. Also shown are the values of effective dose using the phantoms of ICRP-110 and the methodology described in ICRP-103.